

Chaotic oscillation of laser diode with pseudorandom and chaotic signals

Satoshi Ebisawa^{1,2}, Joji Maeda³ and Shinichi Komatsu²

1: Faculty of Engineering, Niigata Institute of Technology
1719 Fujihashi, Kashiwazaki, Niigata 945-1103, Japan

2: Faculty of Science and Engineering, Waseda University
3-4-1 Okubo, Shinjuku, Tokyo 169-8555, Japan

3: Faculty of Science and Technology, Tokyo University of Science
2641 Yamazaki, Noda, Chiba 278-8510, Japan
Email: satoshi_ebisawa@niit.ac.jp

Abstract—We numerically studied the chaotic dynamics of a laser diode (LD) system with optical injection, where an additional signal is applied to the drive current of the master LD. We found that the orbital instability of the LD system is enhanced by applying a pseudorandom signal, and the result showed good agreement that of linear stability analysis. Then we investigated the response of the orbital instability to the frequency range of the applied signal and confirmed a similar trend between this response and the spectrum of the LD system. Moreover, we compared the effect of using a chaotic signal and a band-limited pseudorandom signal having a similar spectrum to the chaotic signal as the applied signal. We showed that the spectrum of the applied signal is a factor affecting the orbital instability of an LD system, and that the use of a pseudorandom signal as the applied signal more greatly enhances the orbital instability than the use of a chaotic signal.

1. Introduction

The oscillation of a laser diode (LD) can be easily made unstable and chaotic by optical feedback from an external cavity, optical injection from another LD, and so forth [1]. If an LD is subjected to optical injection from a chaotic LD, the chaotic dynamics of the two lasers can synchronize (chaos synchronization). Chaotic LDs have potential applications in multiple fields because of their high-frequency oscillation and wide bandwidth. A typical potential application is chaotic secure communication, which has been studied widely, and candidate schemes using chaos synchronization have been proposed [2, 3]. However, it is difficult to protect messages against eavesdropping by a forged receiver using chaotic synchronization.

On the other hand, we have proposed a digital communication scheme that does not depend on chaos synchronization and uses the difference in the orbital instability of a laser system as a binary digit [4]. In this scheme, it is necessary to effectively vary the orbital instability of the laser system to achieve communication without a bit error. In this article, an approach to enhancing the orbital instability of a chaotic optical injection LD system by applying pseudorandom and chaotic signals to the drive current is

numerically described.

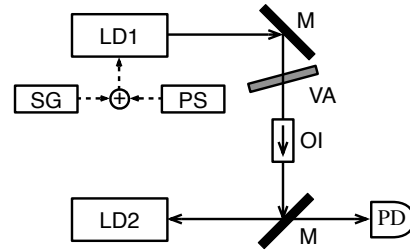


Figure 1: Schematic diagram of chaotic laser system.

2. Optical injection system with applied signal

Figure 1 shows the schematic setup of the chaotic LD system with optical injection, which consists of a master LD (LD1) and a slave LD (LD2). A variable attenuator (VA) is inserted between LD1 and LD2 to control the amount of light injected into LD2. An optical isolator (OI) ensures that LD1 is isolated from LD2. The LDs are pumped by a power supply (PS), and LD1 has a signal generator (SG), which applies an additional signal to the drive current. The dynamical characteristics of LD1 and LD2 without an applied signal can be described by the following rate equations using the complex field $E(t) = A(t) \exp(-i\phi(t))$ and the carrier density above the value for a solitary LD $n(t) = N(t) - N_{sol}$ [5, 6].

$$\begin{aligned} \frac{dA_{1,2}}{dt} = & \frac{1}{2} G_N n_{1,2}(t) A_{1,2}(t) \\ & + \kappa_{inj} A_1(t - \tau_{inj}) \cos[\omega_0 \tau_{inj} + \phi_2(t) - \phi_1(t - \tau_{inj})], \end{aligned} \quad (1)$$

$$\begin{aligned} \frac{d\phi_{1,2}}{dt} = & \frac{1}{2} \alpha G_N n_{1,2}(t) \\ & - \kappa_{inj} \frac{A_1(t - \tau_{inj})}{A_2} \sin[\omega_0 \tau_{inj} + \phi_2(t) - \phi_1(t - \tau_{inj})], \end{aligned} \quad (2)$$

$$\frac{dn_{1,2}}{dt} = (p_{1,2} - 1)J_{\text{th}} - \gamma n_{1,2}(t) - [\Gamma + G_N n_{1,2}(t)]A_{1,2}^2(t). \quad (3)$$

Here, subscripts 1 and 2 denote LD1 and LD2, respectively. The second term on the right-hand side of eqs. (1) and (2) represents the optical injection from LD1 to LD2. G_N , α , γ , and Γ are the differential optical gain, the linewidth enhancement factor, the carrier decay rate, and the cavity decay rate, respectively. The angular frequency of a solitary laser is described as $\omega_0 = 2\pi c/\lambda_0$, where c is the velocity of light and λ_0 is the wavelength. The injection coefficient from LD1 to LD2 is described as $\kappa_{\text{inj}} = (1 - r_0^2)r_{\text{inj}}/r_0\tau_{\text{in}}$, where r_0 is the reflection rate of the incident laser facet, r_{inj} is the fraction of the output of LD1 coupled into LD2, and τ_{in} is the round-trip time in the inner cavity. $p_{1,2}J_{\text{th}}$ is the drive current, where $J_{\text{th}} = \gamma N_{\text{sol}}$ is its value at the solitary laser threshold. In the following section, we consider the case of an additional signal applied to the drive current of LD1. In each case, the average current is modeled so as to be p_1J_{th} . In our simulation, the following values are assigned to the parameters; $G_N = 2.142 \times 10^4[\text{s}^{-1}]$, $\alpha = 5.0$, $\omega_0 = 635[\text{nm}]$, $\gamma = 0.909[\text{ns}^{-1}]$, $\Gamma = 0.357[\text{ps}^{-1}]$, $r_0 = 0.556$, $\tau_{\text{in}} = 8.0[\text{ps}^{-1}]$, $p = 1.11$, $N_{\text{sol}} = 1.708 \times 10^8$, $\tau_{\text{inj}} = 5.0[\text{ns}]$.

In this study, we calculate the exponent, which we call the orbital expansion exponent, from a chaotic laser output to quantify the orbital instability of the chaotic laser. This exponent is calculated by simplifying the method of calculating the Lyapunov exponent proposed by Sato *et al.* [7]. First, the laser output is sampled at intervals of 10ps over 100ns and expressed as $(a_1, a_2, \dots, a_{k-1}, a_k)$. Next, we consider the reconstruction of a phase plane with delay coordinates, i.e., a point on the plane is given as (a_i, a_{i+1}) ($i = 1, 2, \dots, k-1$). We consider the point $(a_{i'}, a_{i'+1})$ ($i' = 1, 2, \dots, k-1$) as a point near (a_i, a_{i+1}) . The distance $\varepsilon_{i,i'}$ between these two adjacent points is assumed to be less than $\bar{a} \cdot 10^{-2}$, and the orbital expansion exponent is described as

$$\lambda = \frac{1}{M} \sum_{\substack{i,i'=1 \\ 0 < \varepsilon_{i,i'} \leq \bar{a} \cdot 10^{-2} \\ i < i'}}^{k-1} \ln \left| \frac{\varepsilon_{i+1,i'+1}}{\varepsilon_{i,i'}} \right|, \quad (4)$$

where M is the number of $\varepsilon_{i,i'}$ satisfying $0 < \varepsilon_{i,i'} \leq \bar{a} \cdot 10^{-2}$.

3. Orbital instability for applied pseudorandom signal

Here, we perform linear stability analysis [1, 8] to consider the steady-state solutions for eqs. (1)-(3), that is, $A_1(t) = A_{1s}$, $A_2(t) = A_{2s}$, $\phi_1(t) = (\omega_{1s} - \omega_{\text{th}})t$, $\phi_2(t) = (\omega_{2s} - \omega_{\text{th}})t$, $n_2(t) = n_{2s}$. From eqs. (1)-(3),

$$\omega_{2s}\tau_{\text{inj}} = \omega_{\text{th}}\tau_{\text{inj}} - \kappa_{\text{inj}}\tau_{\text{inj}} \cdot \frac{A_{1s}}{A_{2s}} \cdot \sqrt{1 + \alpha^2} \sin(\omega_{2s}\tau_{\text{inj}} + \psi), \quad (5)$$

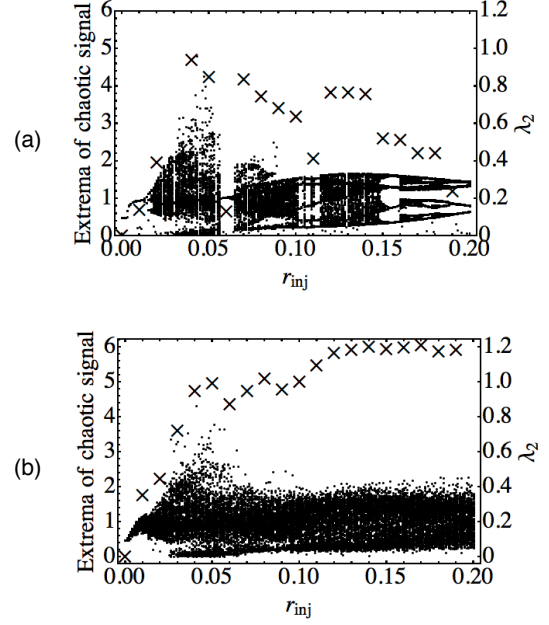


Figure 2: Bifurcation diagram and orbital expansion exponent λ_2 of the LD output versus injection rate r_{inj} . The dots and crosses indicate extrema of intensity and λ_2 , respectively. (a) Bifurcation diagram for LD2 when no signal is applied to the drive current of LD1, and (b) that for LD2 when a pseudorandom signal with $\sigma_1 = 1.0$ is applied to the drive current of LD1.

$$\psi = \tan^{-1} \alpha - \omega_{2s}\tau_{\text{inj}} + \cos^{-1} \left(\frac{-G_{N,2}n_{2s}A_{2s}}{2\kappa_{\text{inj}}A_{1s}} \right). \quad (6)$$

Here eq. (5) is expressed in terms of $\omega_{2s}\tau_{\text{inj}}$, and the solutions correspond to oscillation modes of the laser system. In other words, the stable solutions indicate the points of intersection between the linear function on the left-hand side and the sinusoidal function on the right-hand side. The amplitude of the sinusoidal function depends on the injection coefficient κ_{inj} . If κ_{inj} is sufficiently small, eq. (5) has at most a finite number of solutions, that is, the laser dynamics is expected to exhibit periodic or quasi-periodic oscillation. On the other hand, if κ_{inj} is sufficiently large, eq. (5) has an infinite number of solutions, that is, the laser dynamics is expected to be more complex. Since the number of solutions converges with increasing κ_{inj} , the complexity of the laser dynamics should also gradually converge.

To verify above prediction, the bifurcation diagram plotted against the injection rate r_{inj} is shown in Fig. 2. The dots and crosses indicate extrema of the intensity and orbital expansion exponent λ_2 of LD2, respectively. Figure 2(a) shows the bifurcation diagram for LD2 when no signal is applied to the drive current. For a small injection rate ($r_{\text{inj}} \leq 0.01$), the laser output oscillates periodically and the corresponding λ_2 is small. As the injection rate increases, the dynamics becomes complex and evolves into chaos for injection rates of 0.04 and 0.05, then λ_2 become larger. As r_{inj} is further increased, however, periodic windows within chaotic bands can be observed, whose orbital expansion exponents are small. Although this result appears to contra-

dict the above prediction, chaotic dynamics is observed in the periodic windows by perturbing the phase ψ in eq. (5).

The phase ψ is expressed as a function of the LD1 output A_{1s} , then we modulate the LD1 output by using a pseudorandom signal to perturb the phase ψ . Here, we consider the application of a pseudorandom signal to the drive current of LD1, which is normally distributed with mean $p_1 J_{th}$ and variance σ_1^2 . In our simulations, the signal is generated by the xorshift algorithm [9]. Figure 2(b) shows the bifurcation diagram for LD2 when a pseudorandom signal with $\sigma_1 = 1.0$ is applied to the drive current. For a small injection coefficient ($r_{inj} \leq 0.01$), the laser output oscillates periodically similarly to in Fig. 2(a). As r_{inj} is increased, the dynamics evolves into chaos. The corresponding λ_2 is gradually increased and converges as predicted above. Then the potential chaotic dynamics in LD2 is actualized by applying a pseudorandom signal to the drive current of LD1.

Next, we investigate the frequency response of the orbital expansion exponent to the frequency range of the applied pseudorandom signal. Figure 3 shows the orbital expansion exponent of LD2 plotted against the injection rate r_{inj} . The crosses indicate that no signal is applied to the drive current of LD1. For the other plots, the drive current of LD1 has a band-limited pseudorandom signal filtered by a band-pass filter, which has a Dirichlet window in the range f GHz to $f + 0.5$ GHz. In each case, the average drive current is $p_1 J_{th}$. The orbital expansion exponent λ_2 increases for $r_{inj} > 0.05$ upon applying the signal. When the cutoff frequency is $f = 3.0$ GHz or $f = 4.0$ GHz, it appears that λ_2 is increased by the greatest amount.

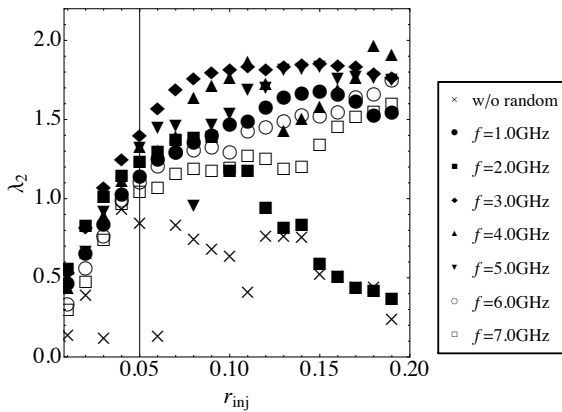


Figure 3: Orbital expansion exponent of LD2 versus injection rate r_{inj} for an applied pseudorandom signal filtered by a band-pass filter within the frequency range f to $f + 0.5$ GHz.

In Fig. 4, the Fourier spectra of chaotic LD2 and the frequency response of λ_2 are plotted in the same plane as that in Fig. 2(b) for (a) $r_{inj} = 0.06$ and (b) $r_{inj} = 0.07$, which are typical cases where the dynamics of LD2 without a pseudorandom signal is a periodic window and chaos, respectively. In each case, the spectrum has a peak at

proximately 3.5GHz and a low power for higher and lower frequencies. The plots of λ_2 have a peak at approximately 3.5GHz, and the distribution of λ_2 is similar to the spectrum of LD2. Therefore, it is expected that the orbital instability can be increased efficiently by applying a pseudorandom signal whose spectrum is similar to the Fourier spectrum of chaotic LD2 to the drive current.

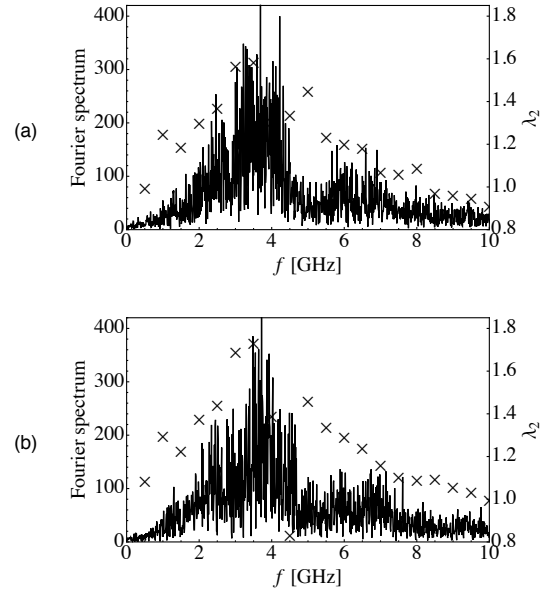


Figure 4: Fourier spectra of LD2 and orbital expansion exponent λ_2 plotted against f when (a) $r_{inj} = 0.06$ and (b) $r_{inj} = 0.07$. Solid lines are Fourier spectra and crosses are plots of λ_2 .

4. Orbital instability for various applied signals

In this section, we investigate factors efficiently increasing the orbital instability of a chaotic LD, then it is clarified whether the applied signal requires chaotic characteristics or only a spectrum similar to that of chaos. Here, we consider three types of applied signal; pseudorandom, chaotic, and complex signals.

The orbital expansion exponent λ_2 plotted against r_{inj} is shown in Fig. 5, where triangles indicate λ_2 without an applied signal and circles, squares, and diamonds indicate λ_2 with complex, pseudorandom, and chaotic signals, respectively. The applied chaotic signal is independent of the dynamics of the LD system in Fig. 1, which is generated by another master-slave LD system with a pseudorandom signal ($\sigma_1 = 1.0$) and a corresponding r_{inj} . The standard deviation of the pseudorandom signal in Fig. 5 is 1.0. The complex signal, which is generated from the pseudorandom signal with $\sigma_1 = 1.0$, is filtered to fit the spectrum of the aforementioned applied chaotic signal. The average drive current for each signal is normalized as $p_1 J_{th}$. For a low injection rate ($r_{inj} \leq 0.05$), in Fig. 5, λ_2 gradually increases with increasing r_{inj} for each signal, but the complex and pseudorandom signals tend to be more effective

for increasing λ_2 than the chaotic signal. This tendency is particularly apparent for $r_{inj} > 0.10$. In this range, λ_2 for the pseudorandom signal remains stable at approximately 1.1. However, λ_2 for the complex signal further increases then converges for $r_{inj} > 0.15$.

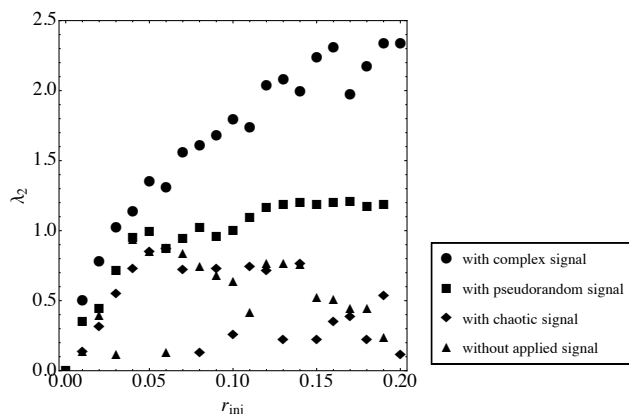


Figure 5: Orbital expansion exponent of LD2 versus injection rate r_{inj} for various applied signals.

Next, the standard deviation of the applied signals is considered. The applied chaotic signal in Fig. 5 has a standard deviation of 0.38. On the other hand, the complex signals generated from the original pseudorandom signals with $\sigma_1 = 0.10, 0.50$, and 1.0 have standard deviations of 0.18, 0.83, and 1.67, respectively. The orbital expansion exponents λ_2 for these applied signals are compared in Fig. 6. When the complex signals are applied, λ_2 increases with increasing value of σ_1 for the corresponding original pseudorandom signal. On the other hand, although the chaotic signal has a larger standard deviation than the complex signal for $\sigma_1 = 0.10$, it has little effect on increasing λ_2 . These findings suggest that a factor that increases λ_2 is the spectral shape of the applied signal and that the property of pseudorandom signal is more important than that of chaos.

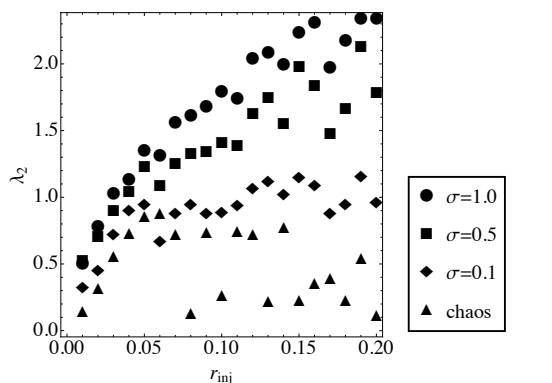


Figure 6: Orbital expansion exponent of LD2 versus injection rate r_{inj} for applied complex signals. σ is the standard deviation of the corresponding original pseudorandom signal.

5. Summary

In this paper, we studied a chaotic system consisting of two LDs (LD1 and LD2) by calculating the orbital expansion exponent to quantify the orbital instability of the dynamics. The output of LD1 is injected into LD2 unidirectionally, and an additional signal is applied to the drive current of LD1. For certain injection rates, periodic windows are observed in the dynamics of LD2, then chaotic dynamics appears upon applying a pseudorandom signal to the drive current of LD1. Then, we considered the effects of applying a pseudorandom signal, an external chaotic signal independent of the entire optical system, and a filtered pseudorandom signal with a similar spectrum to the Fourier spectrum of chaotic LD2, called a complex signal. It is shown that the orbital expansion exponent can be increased more effectively by applying pseudorandom and complex signals than by applying a chaotic signal. In the case of a complex signal, the orbital expansion exponent increases with increasing standard deviation. However, the orbital expansion exponent of LD2 with an applied chaotic signal is smaller, although the chaotic signal has a larger standard deviation than the complex signal. Therefore, it is considered that a pseudorandom signal has a greater effect on enhancing the orbital instability of an LD system than a chaotic signal.

Acknowledgment

This work was supported by JSPS KAKENHI Grant Number JP26790059.

References

- [1] J. Ohtsubo: Semiconductor lasers; Stability, instability and chaos, 3rd Ed.: Springer-Verlag, Berlin (2013).
- [2] R. J. Jones, P. Rees, P. S. Spencer, and K. A. Shore: J. Opt. Soc. Am. B 18 (2001) 166.
- [3] J. Liu, H. Chen, and S. Tang: IEEE J. Quantum Electron. 38 (2002) 1184.
- [4] S. Ebisawa and S. Komatsu: Appl. Opt. 46 (2007) 4386.
- [5] G. H. M. van Tartwijk, A. M. Levine, and D. Lenstra: IEEE J. Sel. Top. Quantum Electron. 1 (1995) 466.
- [6] V. Ahlers, U. Parlitz, and W. Lauterborn: Phys. Rev. E 58 (1998) 7208.
- [7] S. Sato, M. Sano, and Y. Sawada: Prog. Theor. Phys. 77 (1987) 1.
- [8] S. Ebisawa, J. Maeda, and S. Komatsu: in preparation for publication.
- [9] G. Marsaglia: J. Stat. Software 8 (2003) 1.